EPR and EDAX Studies on as-synthesized VO^{2+} doped C3H9Br2CdNo3 single crystal by facile slow evaporation technique and spin Hamiltonian and molecular orbital analysis

N. NITHIYA

Department of Physics,

The Gandhigram Rural Institute-Deemed to be University,

Gandhigram-624302, Tamilnadu, India

P. VICKRAMAN

Department of Physics,

The Gandhigram Rural Institute-Deemed to be University,

Gandhigram-624302, Tamilnadu, India

Abstract

In the present study Vanadium oxide (VO^{2+}), a paramagnetic transition metalion (as a dopant), impregnated into β-alanine cadmium bromide monohydrate (ACBM), a diamagnetic host lattice have been used in different weight ratios to grow well-defined single crystals through slow evaporation technique at room temperature. These as-synthesized single crystals have been subjected to Electron Paramagnetic Resonance (EPR) characterization at three mutually orthogonal crystalline planes i.eab, bc and ca planes. The EPR theoretical and experimental data profile on these samples reveal that single crystals local symmetry is found to be monoclinic and the localization symmetry of the dopant is substitutional affirmed by angular variation and spin Hamiltonian parameters calculations. Further molecular orbital analysis brings forth the energy level of VO^{2+} as it is found to be d ^{22}. The VO^{2+} coordination onto the metal lattice has been understood through spin density function associated with d-electron i.e the dipolar hyperfine coupling constant (P) is found to be 270 , fermi contact term (k) as 0.370 and covalency parameter (α^2) as 0.716 asserts that VO^{2+} localized sharing with metal ligands is of 75% and 25% of it delocalization with later . The complexation of host and guest are confirmed by FTIR and SEM/EDAX.

The as responded EPR single crystal is furtherance subjected to optical absorbance studies by UV-Vis-NIR spectrum and the result shows that there is no absorption found in the entire UV and visible region reveal the optical quality of the ACBM single crystal proves to be a high degree of transparency confirming the NLO nature of the crystal.

Keywords: metal-organic compound; alanine cadmium bromide monohydrate; EPR; spin Hamiltonian parameters.

1. INTRODUCTION

Electron Paramagnetic Resonance (EPR) is a versatile technique to probe into the intricacies of the crystal domain of metal (host) – ion (guest) coordination geometry which brings forth a detailed information about unpaired electron coordination of the guest with the host, its structure, and associated bonding parameters of crystallinity and the corresponding angular variation (orientations of dopant with host in orthogonal planes) involving parameters such as spectroscopic splitting factor (g) and hyperfine splitting factor (A) localization symmetry, revelation provides information about the ground state wave function of paramagnetic ions in different host lattice, dynamic interactions of spins of ions with host lattice (nuclear moments) and site symmetry around the metal ion in a coordinated crystal complex are evolved by this EPR studies. So the researchers have got interest to explore the molecular domain of EPR active materials thereby understanding the applications of crystals in electronic gadgets and optical devices. Consequently researchers delved into probing the paramagnetic transition metal ions based crystals through EPR. Among all paramagnetic transition metal ions, the vanadium is found to exhibit the most stable cationic environment so it has got interest of prominence [1-3].

β - alanine amino acid (organic) which has got a very wide range of applications in material science . This amino acid is optically active in the UV region. When it is forming matrix with metal component (Cadmium bromide monohydrate) it shows interesting NLO properties which has turned the researchers for the new exploration of optical crystals [4]. In this line Renugadevi et al had investigated the crystalline structure of the metal organic amino acid based ACBM single crystal [5]. The recent review show that till date no one has reported the paramagnetic transition metal ion particularly VO^{2+} doped ACBM single crystals by EPR technique.

So in the present investigation the role of transition metal ion in ACBM single crystal has been attempted and results are discussed.

2. MATERIAL SYNTHESIS AND CHARACTERIZATION

To synthesize a single crystal VO^{2+} doped ACBM the pre-cursors β-alanine and cadmium bromide monohydrate (AR grade) are taken in a equimolar ratio (1:1) with VO^{2+} as dopant at different weight ratios. Initially the pre-cursors β-alanine and cadmium bromide monohydrate are dissolved separately in deionized water by continuous stirring for getting a saturated solution. Later VO^{2+} ion is added to the as obtained saturated solution, and the stirring is continued for about five hours for getting a homogeneous solution. This as- obtained homogeneous solution is then filtered by using Whatman filter paper (180 μm) and it is collected into a 2 inch petri dish . The petri dish is sealed tightly using aluminum foil with small holes in it to control the rate of evaporation naturally in dust free environment for the slow evaporation to take place at room temperature for the period of 25 days. Eventually the transparent single crystals of Vo^{2+} doped ACBM well grown crystals formed are subjected to successive recrystallization process to improve the quality of the crystal and as-obtained quality single crystals are subjected to further studies. The same process is repeated for various weight ratios of the dopant. The grown pure ACBM and VO^{2+} doped ACBM are hexagonal in shape with a size of $5\times3\times5mm^3$ and $5\times3\times2mm^3$ respectively as shown in Fig. 1a-1b.
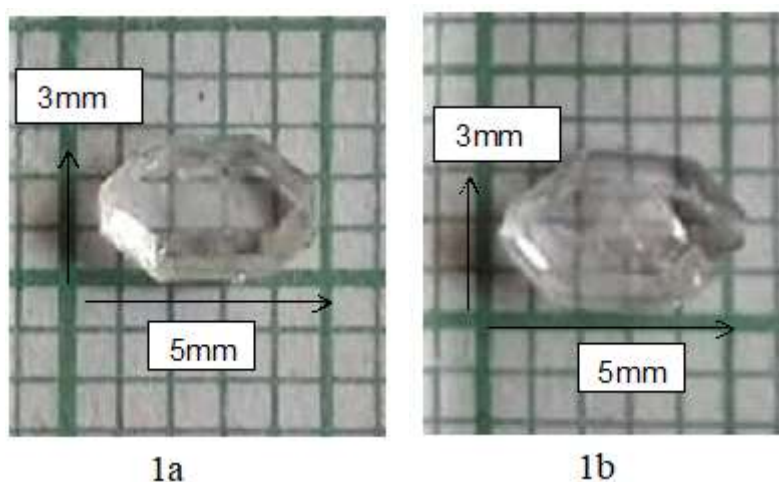

Fig 1: Photograph of pure and VO²⁺ doped ACBM single crystal

3. RESULT AND DISCUSSION

3.1 Single Crystal X-ray diffraction Analysis

As grown Single crystals of pure ACBM, and EPR responding particular weight ratio of VO^{2+} dopant dispersed ACBM have been subjected to SXRD diffractogram studies. The lattice parameters of pure ACBM and impure ACBM have shown no variation in their data profile reveal that both belong to the same monoclinic symmetry with space group P21 [5] as shown in Table1. This suggest that interactive coordination of VO^{2+} guest constituents presence onto a ACBM is not at all disrupting the crystalline geometry of this host lattice.

Table1: Association of Crystal lattice parameters

Lattice Parameters (Pure ACBM)	Single crystal XRD	Single crystal XRD (VO^{2+}-ACBM)
a (Å)	8.673	8.677
b (Å)	13.945	13.948
c (Å)	7.680	7.682
α (°)	90.00	90.00
β (°)	103.71	103.91
γ (°)	90.00	90.00
Volume(Å³)	902.44	910.54
Crystal system	monoclinic	monoclinic Space group
	P2₁	P2₁

3.2   Analysis of EPR Spectral

EPR recording has been carried out for all single crystals grown, at all the three mutually perpendicular directions with $10°$ steps in each plane by rotating the quartz rod (where the single crystal is placed) for different variates of VO^{2+} into ACBM at 9.8 GHz X-band microwave frequency with magnetic modulation of 100 kHz by using Bruker EMX plus spectrometer.

It is noted that among the four different

weight ratios of $(VO^{2+})x$ (X = 0.2,0.5,1,2 gms) in ACBM (1 gm), the VO^{2+}/ACBM in 1:1 ratio has only actively responded to EPR signals so the present investigation is solely upon this particular single crystal analysis. The reason for the response might be the adequate concentration of unpaired electons presence in the outermost orbit inducing paramagnetismin VO^{2+} ion, which is facilitated by host matrix. These unpaired electrons gives rise to well defined eight hyperfine lines in all mutually perpendicular ab, bc and ca planes [6]. One of the recorded hyperfine lines in ca plane at 150° from c axis is shown in the Fig. 2 as an example.
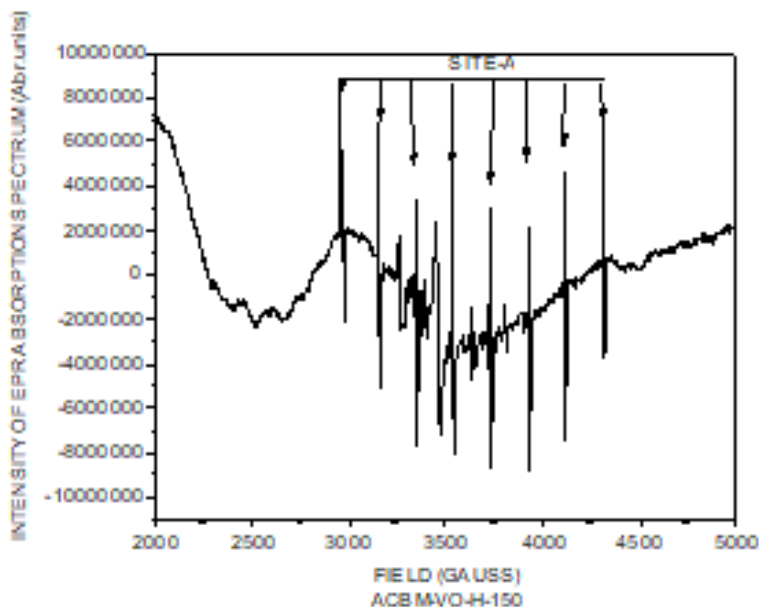
Fig 2: EPR spectrum of VO^{2+}doped ACBM single crystal with magnetic field at an angle 150° from c axis in the ca plane at room temperature.

3.2.1   Angular variation plot and spin Hamiltonian parameters calculation

From the observed eight hyperfine lines associated with ab, bc and ca planes from $0°$ to $180°$ in steps of $10°$ difference, the experimental magnetic field values (H_{exp}) are observed. The theoretical magnetic field values (H_{theor}) can be calculated by using equation (1).

$$H_{theor}=H_{exp}-Km_1 \tag{1}$$

Where H_{exp} is the experimental magnetic field obtained for the eight hyperfine lines

K is the average of experimental magnetic field obtained for the eight hyperfine lines m_1 , is the nuclear-Zeeman splitting value, for VO^{2+} = 7/2

The angular variation graph is drawn between rotational angle Vs magnetic field H_{exp} and H_{theor}, for all the three planes ab, bc and ca respectively as shown in Fig. 3a, 3b and 3c for the well-defined site which consist of a uniformly spaced eight hyperfine line (dotted lines - experimental and solid lines - theoretical). Herein it is referred as site-A (whereas site-B is located but with the merge of these lines so it is ignored in the present study; no trace of site-C is observed in all ab, bc and ca planes). Thus the site-A angular spectra is observed for the planes and the contour of the field positions of site-A in all the planes attributing the anisotropy nature of center meta ion [7-9].
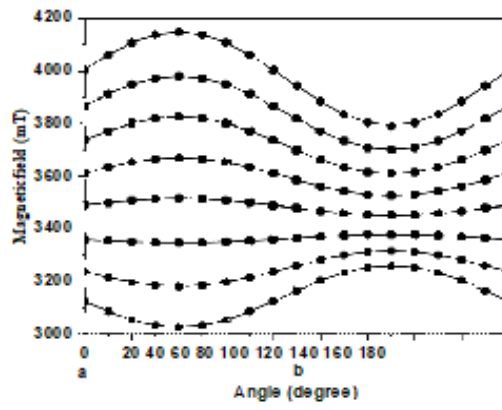
(a)ab-plane
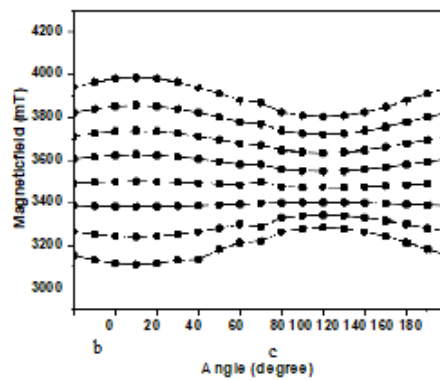
(b) bc- plane
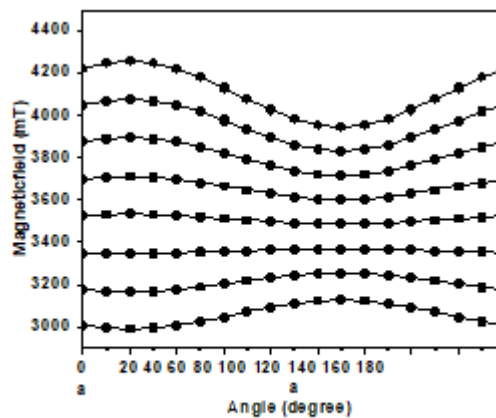
(c) ca-plane

**Fig 3: Angular variation spectra of VO^{2+} doped ACBM of site-A.**

EPR analysis of as-synthesized single crystal of 1:1 weight ratio of dopant and host lattice can well effectively be understood by means of effective spin Hamiltonian parameters (**H**). The spin Hamiltonian parameters for the EPR spectra of VO^{2+} complex is analyzed in terms of an unpaired electrons S=1/2 of VO^{2+} and its nucleus I=7/2 interaction using the equation(2) [7-9].

$$\boldsymbol{H} = \beta S.g.H + A.S.I \qquad \textbf{(2)}$$

(2)

Where β is the Bohr magneton, S is the electron spin vector, g is the spectroscopic splitting factor (g =2.0023 for free electron) and

H is the external magnetic field in Gauss.
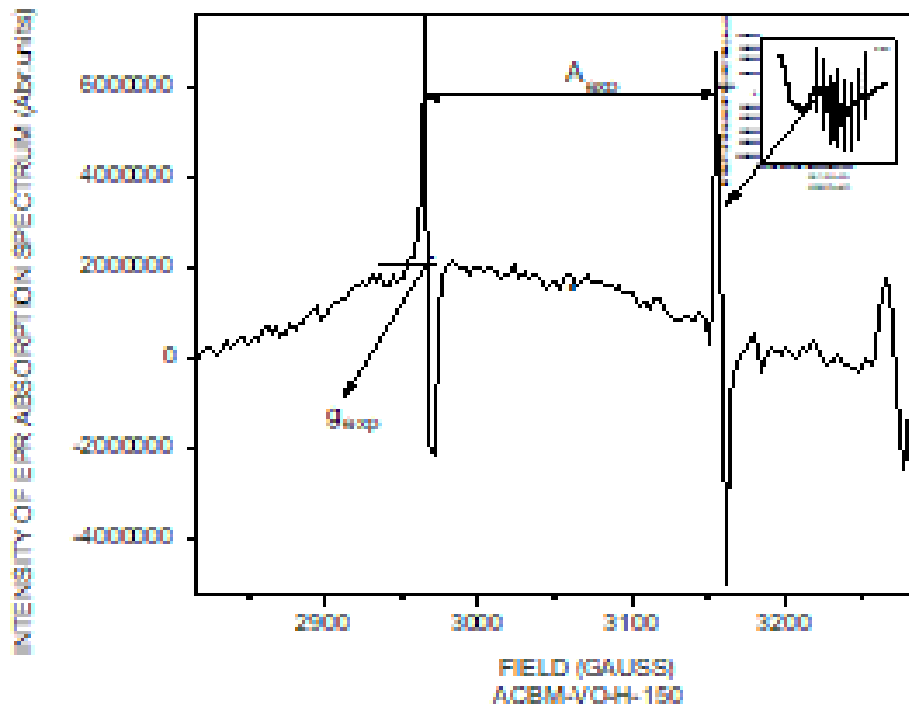
Fig 4: Experimental spectroscopic splitting factor g_{exp} and hyperfine splitting factor A_{exp}.

The experimental spectroscopic splitting factor g_{exp} and hyperfine splitting factor A_{exp} which are, as shown in Fig. 4, providing the interactive mechanism through spin Hamiltonian parameters, are calculated by using the equation (3-3a, 3b) and equation (4).

g_{exp} = $h\nu / \beta H_n$ **(3)**

$(g_{exp})_{max}$ = $h\nu / \beta H_n(\theta_{max})$ **(3a)**

$(g_{exp})_{min}$ = $h\nu / \beta H_n(\theta_{min})$ **(3b)**

$A_{exp} = (H_n - H_1)/(n - 1)$ where n_{max}- eight hyperfine lines, n > 1   **(4)**

The theoretical g_{theor} can be calculated using g_{exp} values and it is fitted with the equation (5).

$(g^2(\theta))_{theor}$ = $\alpha + \beta \cos2\theta + \gamma \sin2\theta$ **(5)**

Where $\alpha = = [(g^2_{exp}).max + (g^2 exp).mini]$ /2

$\beta = [(g^2 exp.)max - (g^2 exp.)mini) \cos 2\theta exp.max]$ /2

$\gamma = [(g^2 exp.)max - (g^2 exp.)mini) \sin 2\theta exp.max]$ /2

When the crystal is rotated from 0° to 180° in all the planes wherein, $\theta_{ex.max}$ is the angle at which $g_{ex.max}$ occurs [7-9]. The A_{theo} can be calculated by using equation (6).

$g^2k(\theta)A^2k(\theta) = g^2_{ii}A^2_{ii}\cos^2\theta i+ g^2_{jj}A^2_{jj} \sin^2\theta j + 2g^2_{ij}A^2_{ij} \sin\theta i \cos \theta j$ **(6)**

(6)

Where g_{ii}, g_{jj}, g_{kk}, A_{ii}, A_{jj} and A_{kk} are the coefficients used to determine the $g^2_k(\theta)A^2_k(\theta)$ in 3 X 3 matrix tensors. The tensors formed are used to obtain the direction cosines associated g tensor and A tensor of the spin Hamiltonian parameters (**H**) [10] Table2.

Table 2: The evaluated spin Hamiltonian parameters (H) for VO^{2+} doped ACBM

Site	g-tensor n		Directional cosines l	m	A tensor n	Directional cosines l		m
A	$g_{xx} = 1.9736$	-0.2691	-0.2652	0.9258	$A_{xx} = 100$	-0.5747	0.8161	-0.059
A	$g_{yy} = 1.9572$	0.9355	-0.3001	0.1860	$A_{yy} = 115$	0.3223	0.2931	0.9000
A	**$g_{zz}= 1.9021$**	0.2285	**0.9162**	**0.3289**	$A_{zz} = 185$	-0.7521	-0.4980	0.4315

3.2.2 Local crystal field symmetry of impurity ion

The EPR studies on host and guest interaction (ACBM and VO^{2+}) is based on g factor symmetry. The g tensor encompasses the three levels of symmetry based on strength of the crystalline electric field and orientation with respect to the axes of the crystal field. If g tensor satisfies the condition, then $g_{xx} \neq g_{yy} \neq g_{zz}$ then the impurity ion is set to experience a weak crystal field which corresponds to orthorhombic symmetry; if g is having the condition $g_{xx} \neq g_{yy} = g_{zz}$ then the impurity ion seems to experience a moderate crystal field which corresponds to axial symmetry, and finally in the third level symmetry g takes the form $g_{xx} = g_{yy} = g_{zz}$ then the impurity ion is subjected to experience a strong crystal field which corresponds to cubic symmetry. In the present investigation the VO^{2+}-ACBM complex show that $g_{xx} \neq g_{yy} \neq g_{zz}$ (Table 2). So the g tensor value in the site-A reveal that VO^{2+} ions exhibits orthorhombic symmetry with the ligands in the host lattice [10-12].

3.2.3 Location of impurity ion and calculation of ground state wave function

The pristine ACBM crystallographic data as reported [5] are used for finding the location of paramagnetic ion (VO^{2+}) in the ACBM crystal lattice .In order to find the location, its g_{zz} tensor values are compared with higher bond length values and the corresponding direction cosines of the center cadmium atom along with respect to its nearest neighbors. It is found that the two directional cosines (m and n values) of g_{zz} almost match with the two directional cosines (l and m values) of **Cd –O2**. Thus directional cosines matching [13 -15] suggest that the VO^{2+} ion locational is substitutional in the ACBM crystal lattice.

Table 3: Directional cosines of center cadmium atoms with respect to its nearest neighbor

Bond	Bond length (A)	Direction cosines		
		l	m	n
Cd–O1	2.420	0.2750	0.8155	0.5190
Cd –O2	**2.358**	**0.9189**	**0.3283**	0.0430
Cd –O3	2.398	-0.2120	-0.4680	0.8590
Cd –Br1	2.617	0.5690	0.5145	0.6450
Cd –Br2	2.664	0.5305	0.3680	-0.7640

To obtain the energy level (ground state wave function) of the substitutional VO^{2+} ion in the host lattice the Rache parameter (R) is employed as given in equation (7).

$$R= (g_{yy}- g_{xx}) / (g_{zz}-g_{yy}) \qquad \textbf{(7)} \qquad (7)$$

In the present study R is found to be 0.2976 which is less than unity, which suggest that ground state nature of the VO^{2+} ion (unpaired electrons) lies predominantly in $d_{x^2-y^2}$ level [16].

3.2.4 Molecular orbital bonding co-efficient: Fermi contact term (k), dipolar hyper fine coupling constant (P) and bonding parameter (α^2)

The Molecular orbital coefficients Pcomplex, k and α perpendicular components of g and A are related to parallel and

of spin-Hamiltonian parameter through the equation (8), (9) and (10).

The calculations of P^{2+} complex, k and α (Table 4) of the substitutional localization of VO lying in the energy state d ^{22} brings forth an strong inference that VO^{2+} ion exhibiting tetragonality distortion (anisotropic) as per the equation (11)

$$\Delta g_{||} / \Delta g_{\perp} = (g_e - g_{||}) / (g_e - g_{\perp}) \qquad \textbf{(11)} \qquad (11)$$

The calculation of (Pcomplex / Pfree-ion) ratio is found to be 25% which representing delocalization of the d- electron and 75% of unpaired spin density of VO^{2+}. The standard literature value of fermi contact term for 3d transition metal ion is 0.36 in the present study it is found to be 0.37 which is thereby confirming the strong EPR signal attribution to 1:1 equal weight ratio of host and guest lattice concentration dependency. The bonding parameter (α^2) is 0.716 indicating that bonding between the metal and the ion is covalent in nature. [18-20].

$P_{complex} = 7(A_{||} - A_{\perp})/6$ **(8)**

Where $A_{\perp} = (A_{xx} + A_{yy}) / 2$, $A_{||} = A_{zz}$,

$P_{free\ ion} = 360 \times 10^{-4}\ cm^{-1}$ [17]   **(8a)**

$k = - (A_{iso} / P_{complex}) - (g_e - g_{iso})$ **(9)**

Where $g_{iso} = (2g_{\perp} + g_{||}) /3$ and $A_{iso} = (2A_{\perp} + A_{||}) /3$

$\alpha^2 = A /0.036 + (g -2.0023) + 3/7(g - 2.0023) + 0.04$ **(10)**
       $||$ $||$ $\perp$

Table 4: Molecular bonding coefficients of VO^{2+}-ACBM single Crystal at room temperature

Complex	$g_{||}$	$g_{\perp}$	g_{iso}	$A_{||}$	$A_{\perp}$	A_{iso}	$(g_e - g_{||})$ / $(g_e - g_{\perp})$	P	k	α^2
ACBM	1.9021	1.9654	1.9443	185	108	134	2.7154	270	0.37	0.716

3.3 FTIR Analysis

FTIR spectra is recorded for the as-synthesized pure ACBM single crystal and VO^{2+} complexed ACBM single crystal in the wavenumber region (finger print region) 1000–400 cm^{-1} as show in the Fig. 5b and 5c. The Table 5 presents the characteristic vibrational bands associated with ACBM crystal and its complex. The host lattice

ACBM bending vibrations in the finger print region have not at all changed either the band positions and the corresponding intensities even with the addition of the vanadium that its presence entangles as doublets at 977 cm^{-1} and 942 cm^{-1} suggest that it is having a surface coordination with ACBM corroborating the SXRD studies and spin Hamiltonian calculations. The functional groups present in the higher wavenumber region are also given as shown in the Table 5 [21-24].
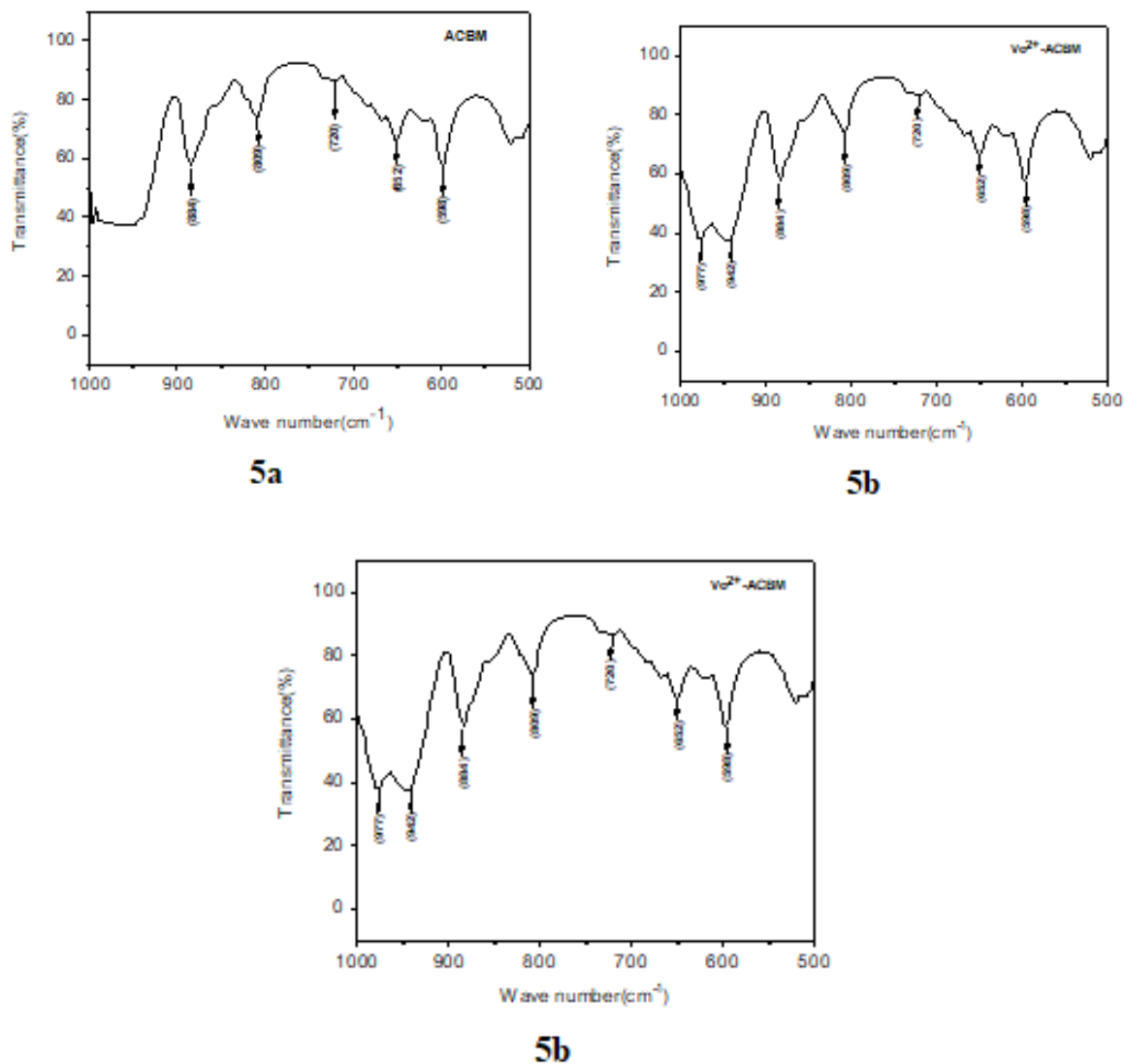
5a

5b

5b

Fig 5: FTIR spectra of pure ACBM (5a); 5b -FTIR spectra VO^{2+} ACBM (400-1000cm^{-1}); 5c-functional group (1000-4000cm^{-1})

Table 5: FTIR of VO^{2+} doped ACBM single crystal

Assignments Mode of vibration	Reported [5] Band in cm^{-1}	Present study Band in cm^{-1}
O–H symmetric stretching	3462	3463
NH$_3^+$ asymmetric stretching	3169	3170
Methylene vibration	1441	1435
C–NH$_2$ stretching	1394	1392
St. NH$_3^+$ rocking stretching	1257	1256
Md.NH$_3^+$ rocking stretching	1112	1115
CN asymmetric stretching	1078	1079
V–O asymmetric	--	977
V–O symmetric	--	942
C–H rocking vibration	--	884
C–H rocking vibration	--	809
C–H rocking vibration	--	720
C–Br bending vibration	--	652
Cd–O bending vibration	--	598

3.4 EDAX Analysis

The compositional mapping of the constituents of as grown pure ACBM single crystal and impure ACBM single crystal (of EPR response) are recorded and compared by EDAX and reveal that

the strong presence of VO^{2+} is shown in Fig with strong tiny contour (a new appearance, and shooting up heights of pure ACBM after the dispersion of VO^{2+} are (distinctly seen) confirming conjoining complexation of VO^{2+} with ACBM [20].
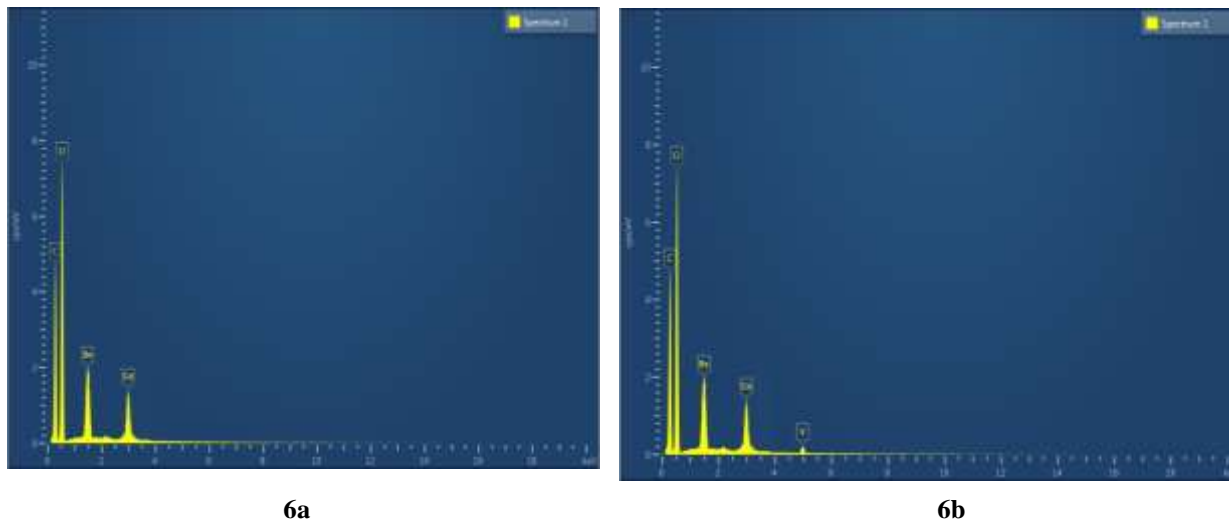

| 6a | 6b |

Fig 6: EDAX Spectrum of Pure ACBM (6a) and VO^{2+} doped ACBM (6b) single crystal.

Table 6: EDAX quantification of Pure and VO^{2+} doped KBDC single crystal

S. No	Elements	Wt% (Pure)	Wt% (Doped)
1.	C	40.10	40.10
2.	O	52.14	52.14
3.	Br	4.21	4.21
4.	Cd	3.05	3.05
5.	V	---	0.5
	Total	100	100

3.5 UV-Vis-NIR Spectral analysis

The optical absorption spectrum of ACBM single crystal have been recorded by using Perkin Elmer lamda-35 UV-VIS-NIR spectrometer with wavelength range between 190 - 1100nm at room temperature. The wide range of transparency of any material can be found out using UV-Vis-NIR Spectral analysis. The absorption spectrum of the grown sample is recorded between 190-1100 nm and it has lower cut off wavelength at around 225nm. It is observed that the absorbance is not registered till the wavelength reaches 205nm. At that wavelength, a sudden fall of transmittance was observed which shows that only a single transition occurs in the near UV region. Thus the sharp fall in transmittance suggest that the even distribution of energy takes place in all the molecules of ACBM single crystal. A UV-Vis-NIR spectrum of the grown crystal is shows in the Fig. 8. It shows that there is no absorption in the entire UV and visible region means a high degree of transparency proves the optical quality of the grown ACBM single crystal [25].
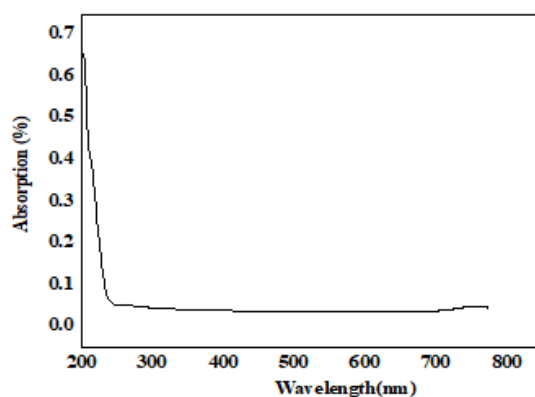
Fig 7: Optical Absorption Spectrum of ACBM NLO single crystal

3.6 CONCLUSION

➢ SXRD studies on unit cell parameters calculation reveal that pristine ACBM and VO^{2+}dispersoidACBM single crystals are found to have orthorhombic symmetry.

➢ The EPR Signal maximum absorption has been observed for 0.5gof VO^{2+} impurity in ACBM.

➢ The angular variation calculation through spin Hamiltonian parameters such as spectroscopic splitting (g) tensor values and hyperfine splitting (A) tensor values confirming the SXRD results and in concurrence with Jorgensen field theory on local field symmetry.

➢ The bond length Cd–O_2 and the direction cosines of g_{zz}-tensor values have good agreement with each other confirming the impregnation of VO^{2+} ion as substitutional.

➢ ThemolecularorbitalanalysisthroughRacheparameterwhichconfirmstheVO^{2+} prevailing presence between ionic and covalent.

➢ The FTIR study confirms complexation of VO^{2+} through its presence at fingerprint region.

➢ SEM and EDX image profile has not shown any major difference in all magnifications.

➢ However the EDX confirms its presence through the level of absorption by VO^{2+} in the impure ACBM crystal.

REFERENCE

[1] Ram Kripal, Anurag Mishra, Chemical Physics Letters 478 (2009)307–309.

[2] Juliet Sheela K, Radha Krishnan S, Shanmugam V M, Subramanian P, j.molstruc 1131(2016)311619.

[3] BunyaminKarabulut, AyseTufan, SpectrochimicaActa Part A 65 (2006)742–748.

[4] Chandrasekaran J, Ilayabarathi P, Maadeswaran P, Rasayan.J.Chem 2 (2011) 425 –430.

[5] Renugadevi R, Kesavasamy R, J.Phase transition 87 (2014)881-892.

[6] ZeynepYarbas, BunyaminKarabulut, AbdulhalikKarabulut, j.physb 404 (2009) 3694– 3697

[7] Subramanian P, Juliet Sheela K , Radha Krishnan S , Shanmugam V M,j.molstruc. 1206 (2020) 127586.

[8] Schonland D S, Proc. Phys. Soc, 73 (1958) 788-792.

[9] Abragam A and Bleaney B, Electron Paramagnetic Resonance of TransitionIons, Clarendon Press, Oxford (1970)133.

[10] Karabulut B, Düzgün F, Spectrochim. Acta**A75**(2010)1200–1202

[11] Dwivedi P, Kripal R, Misra M G, J. Alloy. Compd. **499**(2010)17–22

[12] Poonguzhali E, Srinivasan R, Venkatesan R, Ravikumar R V S S N, Rao P S, J.Phys. Chem.Solids**64** (2003) 1139–1146

[13] Suryanarayana D and Sobhanadri J, J. Magn. Reson.14, 1(1974).

[14] Juliet sheelaK, Radha Krishnan S , Shanmugam V M, Subramanian P,j.molstruc. 1158(2018) 66-74.

[15] Subbulakshmi N, Juliet Sheela K, Subramanian P, Single crystal EPR studies of Cu^{2+}ion doped lithium potassium phthalate, AIP Conference Proceedings **1832**, (2017)100009.

[16]   Srinivas D, Swamy M V B L N, Subramanian S, Mol. Phys. **57**(1986)55–63.

[17]   Selvakumar P N, Natarajan B, Sambasiva Rao P, and Subramanian P Cryst.Res. Technol, 43 (2008) 857 – 862

[18]   Gangadharmath U B, Annigeri S M, Naik A D, Revankar V K, Mahale V B, J.Mol. Struct 572 (2001) 61.

[19]   Prochaska J J, Schwindger W F, Schwartz M, Burk M H, Bernarducci E, Lalancette RA, Potenga J A, Schugar H J, J.Am.Chem.Soc103 (1981)3446.

[20]   Jorgensen C K, Modern aspects of crystal field theory (North-Holland PublishingCo, Amsterdam)1971.

[21]   John Coates ,Ency.Anal. Chem (John Wiley & Sons, Ltd)2006.

[22]   Derek Peak, George Luther W, Donald Sparks L, GeochimicaetCosmochimicaActa67 (2003)2551–2560.

[23]   Enrique J, Barana and Kwang-Hwa Liib, Naturforsch. 58b (2003)485–488.

[24]   Varghese Mathew, Jochan Joseph , Sabu Jacob, Varughese P A and Abrahm KEIndian.j.pure&applphys47(2009)691–695.

[25]   Banuchitra S, AlagaM, Int. Jour. Res. App. Sci. Eng& Tech ,3 (2015)2321-9653.